

## Seismic assessment of historical masonry construction including uncertainty

Yiannis Petromichelakis<sup>1</sup>, Savvas Saloustros<sup>2</sup>, Luca Pelà<sup>2</sup>

<sup>1</sup> M.Sc. Institute for Structural Analysis, Technische Universität Dresden, 01062 Dresden, Germany.

<sup>2</sup> Technical University of Catalonia (UPC), Campus Norte, Jordi Girona 1-3, 08034 Barcelona, Spain.  
email: yiannispetro@gmail.com, savvas.saloustros@upc.edu, luca.pela@upc.edu

**ABSTRACT:** The evaluation of the seismic vulnerability in monumental buildings is a complex task. This is due to the inherent uncertainty of ancient structures regarding their structural characteristics and material properties that should be properly handled in their seismic assessment. Consequently, a probabilistic study considering the material and structural uncertainties is a necessary step for the seismic protection of the built cultural heritage. This paper presents the study of the seismic vulnerability of the church of the Poblet Monastery, an UNESCO World Heritage Site in Spain. The seismic capacity was studied using a Finite Element model of a selected damaged bay of the church by means of a pushover analysis. The nonlinear behaviour of masonry is described by a continuum damage model improved by a tracking technique representing the localization of cracks and the consequent activation of the collapse mechanism. A Monte Carlo simulation enhanced by the Latin Hypercube Sampling technique was utilized to estimate the effect of the uncertainties, regarding the material and structural characteristics, on the seismic performance of the structure. The developed fragility curves express the safety level and the damage expected on the structure for different seismic scenarios.

**KEY WORDS:** Masonry, Continuum damage model, Localized cracking, Uncertainty, Monte Carlo simulation, Latin Hypercube Sampling, Fragility curves

### 1 INTRODUCTION

Ancient masonry constructions form a very important part of the tangible cultural heritage. They constitute records of the history and the building technology of different cultures and encompass important artistic heritage (e.g. frescoes, mosaics). Additionally, in many cases they still form a part of the servicing infrastructure of the modern communities by either maintaining their original use (e.g. churches, bridges) or acquiring new one (e.g. museums).

Masonry structures with structural integrity under gravitational loads may demonstrate a very low capacity against earthquake, even of low intensity. This fact was dramatically validated during the recent earthquakes in Emilia-Romagna in Italy (2012) with the majority of damaged and collapsed structures being churches. Therefore, it emerges the necessity to evaluate the seismic safety of monumental buildings.

Unlike to modern structures, the structural analysis of ancient ones is hampered by a sufficient amount of uncertainty, mainly due to the deficient mechanical characterization of materials. The reduction of this uncertainty requires in-situ and laboratory investigations that are usually limited due to costs and common restrictions for interventions on monuments. Consequently, the comprehensive study of a historical construction should incorporate a methodology for the consideration of uncertainties in the structural parameters, as well as their probable intervals of variation.

This paper presents the seismic vulnerability of an important monument of Spain, the church of the Poblet monastery, including uncertainties in material and structural properties. For the purposes of the analyses a two-dimensional (2D) Finite Element (FE) model of a chosen bay of the church

was developed. A continuum damage model with a tracking algorithm was used for the representation of the crack localization. The uncertain material parameters that can influence the structure's seismic response were taken into consideration with the aid of random variables. A Monte Carlo Simulation (MCS) improved by the Latin Hypercube Sampling (LHS) technique was employed to propagate the uncertainties in the material properties of the masonry. Three damage states in agreement with the structure's damage under horizontal actions were defined and their probability of occurrence was evaluated with the development of fragility curves.

### 2 THE CASE STUDY

The case under study is the church of the Royal Monastery of Santa Maria de Poblet, located in the municipality of Vimbodí and Poblet, in Spain (Figure 1). The whole construction forms a very important part of the country's built cultural heritage. In 1921, the Spanish government recognized the whole complex as a national monument and since 1991 it is an UNESCO World Heritage Site.

The construction of the church took place between 1170 and 1276, starting with the eastern part (i.e. the apse, its surrounding chapels and the transept) and finishing with the main nave and the two aisles in the western part. Its present morphology differs from the original due to the demolition and reconstruction of the southern aisle and its adjacent chapels (left in the transverse section in Figure 2) in the 14<sup>th</sup> century, which led to the non-symmetrical geometry of the lateral aisles. The cimborio over the transept is an addition of the 15<sup>th</sup> century.

The church presents today significant damage affecting the main and lateral naves. The clerestory walls present an outwards rotation with the horizontal displacement at the springing of the barrel vault having values above 10 cm. Moreover, the barrel vault presents a deflection increasing up to 50 cm in the bay under the 5<sup>th</sup> arch (with respect to the transept). Cracking near the key of the vaults is evident both in the main and lateral naves.



Figure 1. The church of the Royal Monastery of Santa Maria of Poblet: (a) external view and (b) internal view.

A past study on the church [1] showed that the geometry of the structure, mainly characterized by the irregularity in elevation, together with the structural alteration of the 14<sup>th</sup> century and a past seismic action may have induced the present damage. However, even if the estimation of the causes of the damage in the structure was possible, the uncertainty affecting the structural and mechanical parameters of the materials hamper the assessment of the seismic capacity. These difficulties, common in the study of built cultural heritage, are addressed in the current study with the utilization of the methodology presented in Section 3.

### 3 METHODOLOGY FOR THE SEISMIC ASSESSMENT OF THE MONUMENT

#### 3.1 Finite Element analysis

In the study of historical constructions the modelling of the whole structure is a very demanding process that requires an exhaustive survey. The composing parts of the structure show a different response under an earthquake, especially in churches where the connections between members are usually not effective [2]. Consequently, the identification and study of the most important collapse mechanisms can be performed separately by considering representative macroelements [3].

In the current work, the evaluation of the seismic performance of the western part of the church (i.e. main and lateral naves) is performed, since such macroelement is already damaged and may be rather vulnerable to an earthquake. For the purposes of the structural analysis, a plane-stress model of the frailest bay of the church was designed. The model represents the actual deformed geometry, derived with a laser scanner survey (Figure 2), of the bay under the fifth arch (with respect to the transept) that

exhibits the highest deflection of the barrel vault and lacks a flying buttress at its southern part.

The two dimensional model (2D) was based on the detailed three-dimensional (3D) FE model of the same bay presented in [1]. Both models show equal weight of the different structural elements, equivalent deformed shapes after non-linear analysis for the action of the self-weight and equivalent seismic response after a pushover analysis. The consistency of the results between 2D and 3D FE models, in cases where three-dimensional effects are not influential, has been demonstrated in previous studies [4], [5] and [6].

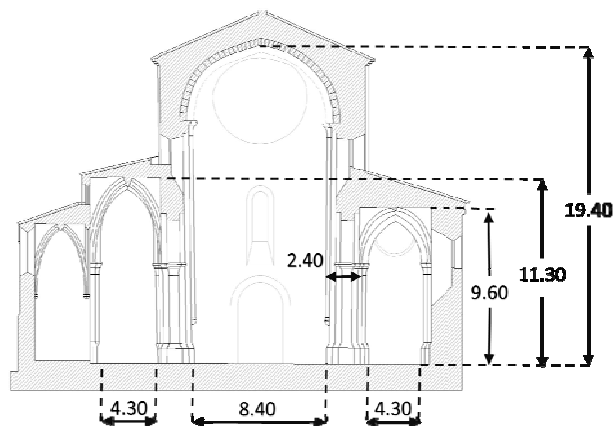


Figure 2. Transversal section of the bay under investigation.

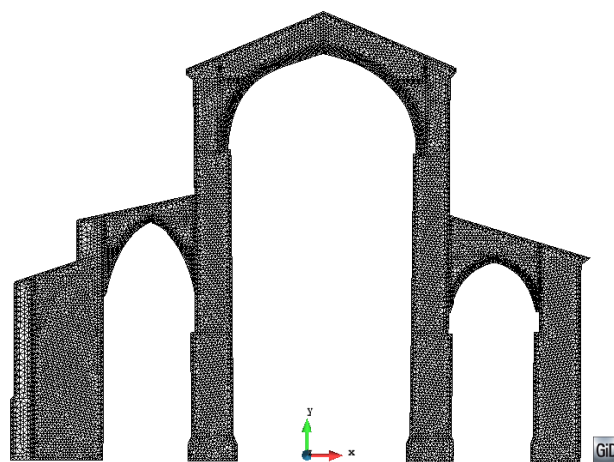


Figure 3. The adopted FE mesh.

The seismic performance of the macroelement was evaluated with the use of a non-linear static analysis (i.e. pushover analysis). The pushover analysis can provide important information on the collapse mechanism and the capacity of the investigated structure and has been included in recent codes [7], [8] and [9].

The material behaviour is represented with the use of an enhanced continuum damage model that can describe the tensile crack localization by means of a local tracking technique [10]. This model can represent effectively the seismic behaviour of masonry buildings [11]. The initiation and propagation of discrete cracks is properly represented, until the activation of a mechanism in which the structure is

composed by blocks separated by localized cracks. In this way, the analyst can follow the structural behaviour from the activation of the mechanism, through its development and until the collapse.

Figure 3 illustrates the adopted FE mesh which is composed by 20093 triangular elements and 10863 nodes. The pushover analysis was carried out in two steps: firstly the dead load is applied to the structure and secondly the seismic action is represented with an incremental increase of the horizontal forces, proportional to the mass distribution, until reaching the maximum capacity. It is noted that the performed analyses include the effect of geometrical non-linearity. The pre- and post-processing was performed in GiD [12] and the analyses with COMET [13], developed by CIMNE in Barcelona.

### 3.2 Damage grades

In the seismic assessment of a structure it is common to investigate different *damage grades* representing the various performance levels during the lateral loading, until determining the ultimate capacity. In a territorial seismic assessment of a population of buildings, varying in structural typology and material properties, it is usual the adoption of a simplified methodology for the determination of the damage thresholds. Some studies define such thresholds as a function of the yield displacement of the idealized pushover capacity curves [14]. However, when dealing with a specific construction typology a more precise definition of the damage thresholds is more useful. The EMS-98 [15] has proposed five damage grades for unreinforced masonry buildings depending on the damage observed in structural and non-structural elements. This methodology has been adopted by different researchers in the past years for the assessment of unreinforced masonry structures with some modifications for the better adoption in each studied case, see [16] and [17].

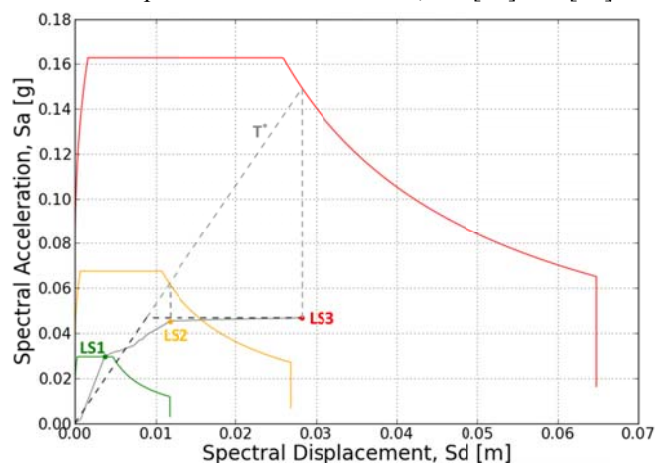


Figure 4. Methodology for obtaining the demand in terms of PGA for each of the limit states.

The present work follows the latter philosophy and three damage grades were defined according to the damage observed to the structure during its lateral loading. Figure 4 illustrates a generic capacity curve of the church for one of the studied cases. The capacity curve is characterized by three different damage thresholds. Each of them corresponds to a different *limit state* caused by the onset and propagation of

new damage and therefore the reduction of the structural stiffness.

Figure 5 presents the respective damage level in the structure for every different limit state. The structure under its self-weight presents cracking at the intrados of the vaults in the lateral aisles, at the extrados of the northern aisle (right aisle as presented in the figures) and the extrados of the barrel vault in the main nave (Figure 5a). During the application of the lateral loading, the cracking in the northern lateral aisle is the first to propagate. The first threshold in the obtained capacity curve (point LS1 in Figure 4) refers to the onset of cracking near the key of the barrel vault in the main nave and the rotation of the external wall in the northern aisle (locations highlighted by green circles in Figure 5b). This first loss of stiffness of the structure due to the respective damage is defined as the limit-state 1 (LS1). The second branch of the capacity curve, between points LS1 and LS2, refers to the propagation of the already opened hinges (three in the main nave and three in the lateral aisle) and the initiation of the rotation of the pier in the main nave (Figure 5c). The corresponding limit state is reflected in the capacity curve as the second loss of stiffness (point LS2 Figure 4). Finally, the collapse occurs when the rotation of the pier of the main nave is high enough to lead to the opening of all the hinges in the main nave and lateral aisle (Figure 5d and point LS3 in Figure 4).

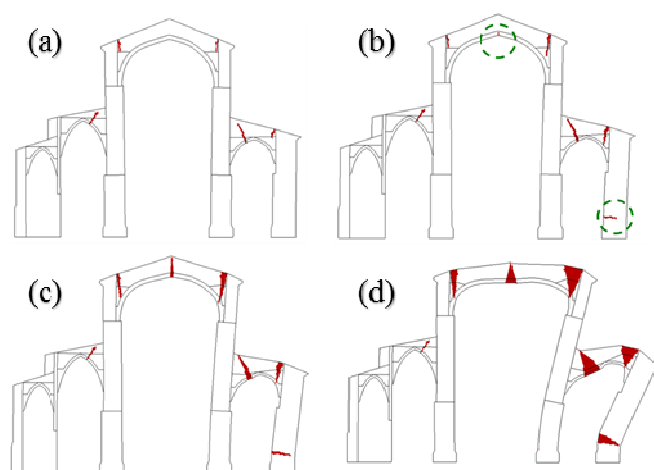


Figure 5. Deformed shape and tensile damage distribution of the structure for: (a) self-weight, (b) first limit state (LS1), (c) second limit state (LS2), and (d) third limit state (LS3).

### 3.3 Seismic assessment

Figure 6 presents the procedure for the seismic evaluation of the investigated structure. The obtained capacity curves of the multi degree of freedom structure were transformed to the equivalent single degree of freedom system and subsequently to the equivalent bilinear (elastic-perfectly plastic) curve. Thereafter, the displacements of each of the limit states were compared with the yield displacement of the idealized curve. If a limit state has a displacement lower than the yield displacement, the structure is considered to be still in the elastic range. Therefore, the seismic demand, in terms of peak ground acceleration, is identified by the corresponding elastic response spectrum intersecting the performance point on the capacity curve for the specific limit state. On the other hand,

for the limit states with displacement higher than the yield displacement the N2 procedure, as it is included in the Annex B of the Eurocode 8 [7], was followed. Once the performance of the structure is established in terms of damage levels, the N2 method allows us to determine the corresponding seismic demands, expressed by inelastic spectra. Figure 4 shows the operation to determine the seismic demands at the performance points LS2 and LS3. The elastic spectrum used was the one proposed by the EC8 for the soil characteristics of the area, which is a cohesionless material referring to type of Soil D. It is noted that the location of the control displacement is considered the top of the structure (key of barrel vault) as suggested by the N2 method and followed in studies of similar constructions [18] and [19].

### 3.4 Uncertainty in the material properties

Up to date, limited information is available regarding the properties of the composing materials of the church. The masonry is made of limestone, the prevalent material used in almost all the buildings within the monastery, obtained from local quarries. A detailed investigation in 2012 in the infill of the barrel vault over the central nave revealed its composition of very poor quality material with non-structural characteristics.

Deterministic values for the mechanical properties of the masonry were obtained in accordance with the in-situ inspection and following the suggestions of [20] and [21]. However, due to the limited information and experimental data regarding the masonry of the church, these values are uncertain. Deviation of the real values of the mechanical properties from the adopted deterministic ones is possible and can be attributed to either *natural variability* or to *impreciseness* of information. Uncertainty related to natural variability (randomness) is called *aleatoric*, while uncertainty related to lack or impreciseness of information is called *epistemic* [22]. Additionally, epistemic uncertainty arises due to the fact that it is commonly not definite that the numerical models treat the material parameters in accordance with their real physical significance.

Consequently, in this work the adopted methodology assumes that the mechanical properties of the masonry vary within a specified range with the aforementioned deterministic values as central values.

### 3.5 Uncertainty modelling

Different mathematical models have been developed to assess uncertainty characteristics within a computational framework [23]. The most convenient by means of effectiveness,

simplicity and numerical efficiency, adopts the concept of *random variables* derived from probability theory to assign uncertainty characteristics to the uncertain parameters.

Six uncertain parameters have been taken into account and modelled as random variables (Table 1). Five refer to the material properties of the masonry, i.e. the compressive strength  $f_c$ , the tensile strength  $f_t$ , the Young's modulus  $E$ , the density  $\rho$  and the tensile fracture energy  $G_f$ , and one, the coefficient  $I_{coeff}$ , refers to the infill of the lateral vaults, where no information is available regarding its consisting material. The intervals of variation of the uncertain parameters were obtained in accordance with values suggested by [20] and [21] for masonry typologies similar to that of the investigated church. The mechanical properties of the infill are considered equal to a percentage of the corresponding masonry properties according to the coefficient  $I_{coeff} \leq 1.0$ . It is noted that the density of the infill is considered equal to the density of the masonry in all simulations.

The parameters  $f_c$ ,  $f_t$ ,  $E$ , and  $\rho$  possess aleatoric and epistemic characteristics simultaneously. Due to the fact that it is more likely that the real values of these material properties lie close to the initially adopted deterministic values, normal distributions were assumed for  $f_c, f_t, E$ , and  $\rho$ , see Table 1.

The parameters  $I_{coeff}$  and  $G_f$ , on the other hand, possess epistemic uncertainty. Experimental data about them is unavailable and only rough assessments about their variation intervals can be provided. For that reason, uniform distributions define the corresponding random variables in this work.

Table 1. Random Variables.

	Mean Value	c.o.v*	Distribution	Units	Uncertainty**
$f_c$	4.0	12.5%	Normal	MPa	A, E
$f_t$	0.2	20%	Normal	MPa	A, E
$E$	2000	12.5%	Normal	MPa	A, E
$\rho$	2100	4.8%	Normal	kg/m <sup>3</sup>	A, E
	Min	Max			
$G_f$	10	100	Uniform	J/m <sup>2</sup>	E
$I_{coeff}$	0.2	1.0	Uniform	-	E

\* c.o.v = coefficient of variation

\*\* A = aleatoric, E = epistemic

### 3.6 Uncertainty analysis

The effect of the uncertain parameters, modelled as random variables, on the seismic response of the complex masonry structure can be evaluated by utilizing stochastic simulation. In this approach, the quality of the solution is affected by the trade-off between accuracy and numerical efficiency; the

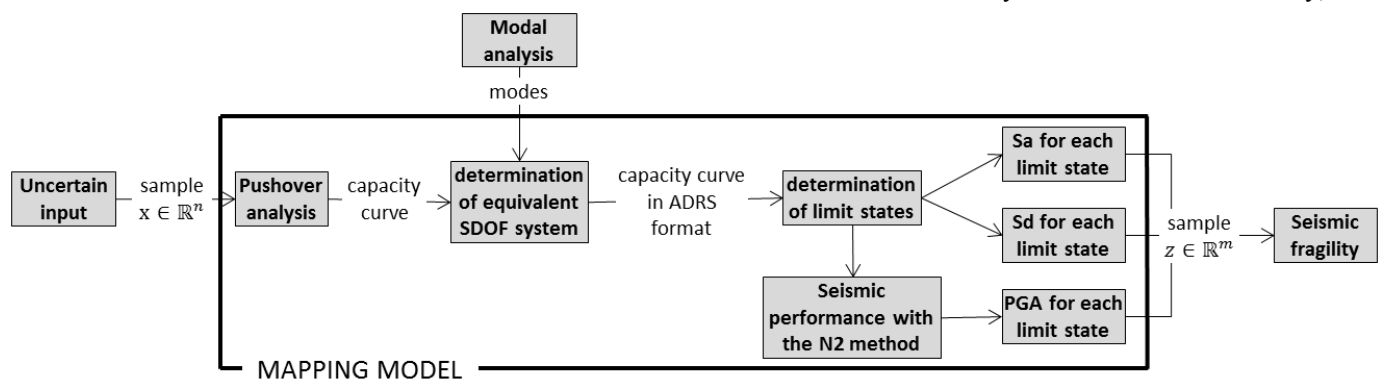


Figure 6. Schematic view of the adopted methodology.

validity of stochastic methods is provided by statistical laws (Central Limit Theorem and Strong Law of Large Numbers [24]), which require the number of samples  $N$  to approach infinity,  $N \rightarrow \infty$ . Consequently,  $N$  should be sufficiently large, a condition that is problem dependent and highly influenced by the number of uncertain parameters. The most convenient but at the same time the most computationally expensive among the stochastic methods, is the Monte Carlo Simulation, which has been adopted in similar studies, [25] and [26].

The Monte Carlo Simulation (MCS) method generates a specified number of  $N$  independent and identically distributed (i.i.d.) random samples within the input space  $\mathbf{X} \subseteq \mathbb{R}^n$ , where  $n$  is the number of random variables. Each random variable is distributed according to a specified probability distribution, which is taken into account in the sampling process. Subsequently, a mapping model (Figure 6) maps each sample to the result space  $\mathbf{Z} \subseteq \mathbb{R}^m$ , where  $m$  is the number of the result variables that need to be evaluated. In this study the  $m$  result variables are the spectral acceleration ( $S_a$ ), spectral displacement ( $S_d$ ) and peak ground acceleration ( $PGA$ ) for each one of the three limit states (i.e.  $m = 9$ ).

Namely, MCS creates a population of  $N$  possible instances of the structure, each of which needs to be analyzed. As a result, under the assumption that  $N$  is large enough, this methodology provides full insight on the distributions of the result variables that describe the seismic performance of the structure.

An improvement in the efficiency of the MCS can be achieved by employing the Latin Hypercube Sampling (LHS) method proposed in [27]. LHS is a special case of stratified Monte Carlo sampling that reduces the variance of the standard MCS. According to [28], the standard error of the LHS declines with a rate of approximately  $\sqrt{N^3}$  for linear functions, while in the standard MCS the corresponding rate is much lower, it approaches the value  $\sqrt{N}$ . Thus, despite the fact that the functional behaviour of the seismic response of a masonry structure is far from linear, the total number of simulations can still be sufficiently reduced by the use of the LHS method. The minimum sample size, appropriate to produce statistically acceptable results with respect to the number of random variables, is still an open subject. In the current study, a number of  $N = 200$  was selected in accordance with [29] and [30].

## 4 RESULTS

### 4.1 Capacity curves

Figure 7 shows the 200 obtained capacity curves in terms of spectral displacement ( $S_d$ ) - spectral accelerations ( $S_a$ ), as well as the 16%, 50% and 84% fractile curves. The significance of the side fractile values (16% and 84%) is their coincidence with the values of the mean  $\pm$  the standard deviation [31]. Through this illustration it is possible to have a coarse estimation of the most probable (68% probability) range of variation of the capacity curve, which lies between the boundary determined by the 16% and 84% fractile curves. It is visible that the variation of the properties affects significantly the capacity of the structure, whereas the variation in the elastic part is comparatively low.

Figure 8 presents the mean and the median (50% fractile) capacity curves, together with the pushover curve of the reference case which depicts the capacity of the structure for the mean values of the uncertain parameters shown in Table 1. The slightly higher elevation and extension of the mean curve compared to the median, implies that for each displacement the mean value of the curves above the median are located slightly farther from the median than the respective curves below. This is more evident in Figure 7, where the curves above the median appear significantly more dispersed than the curves below, especially in terms of spectral acceleration. Consequently, for the adopted distributions of the uncertain parameters, for given  $S_d$  the distribution of  $S_a$  is unsymmetrical and shifted to the lower values (i.e. positive skewness).

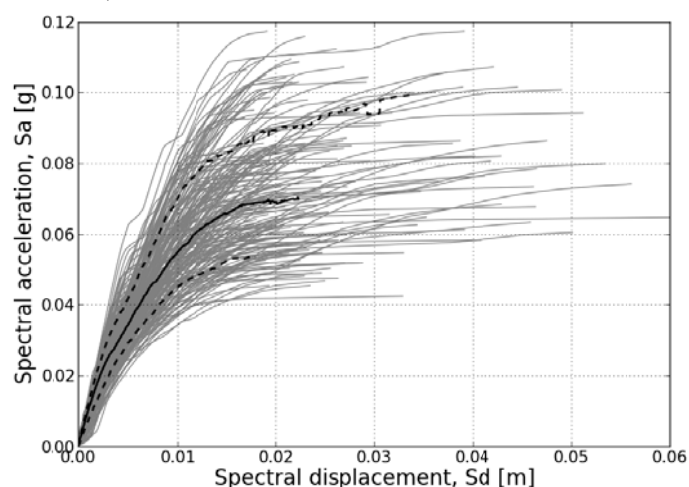


Figure 7. The obtained capacity and 16%, 50% and 84% fractile curves for the 200 performed pushover analyses.

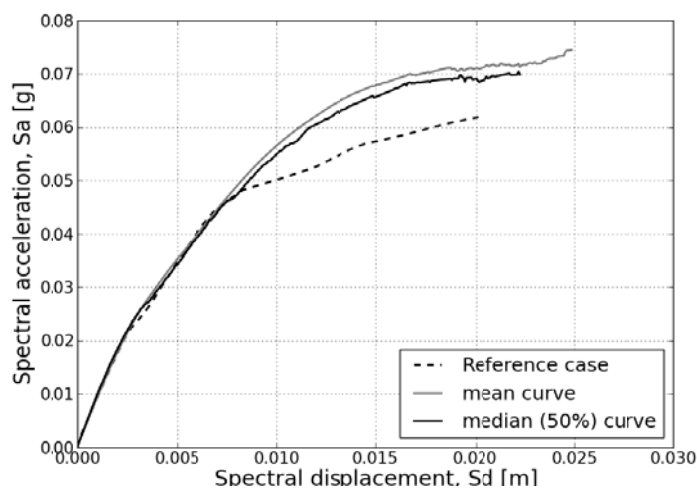


Figure 8. Mean, median and reference case capacity curves.

A similar conclusion can be drawn by looking at the position of the capacity curve for the reference case (mean values of the uncertain parameters) in Figure 8. The difference between the mean and the reference curve implies an unsymmetrical influence of one (or more) input parameter to the structural capacity. More specifically, samples of this input parameter that are above the mean, push the capacity curve upwards more than the samples below the mean push it downwards. Consequently, it can be interestingly derived that

the adoption of the mean values as input for the uncertain parameters, can lead to significantly conservative results regarding the structure's capacity. This result motivates the purpose of this work and stresses the importance of the analysis of uncertainties in the seismic assessment of the church.

#### 4.2 Statistical results for each limit state

It is more convenient to express the variability in the results using arithmetic terms. This can be achieved by estimating specific moments of the distributions of the calculated capacities  $S_a$  and  $S_d$  or for the corresponding demands in terms of PGA, for each limit state. For the purpose of the present work, it is reasonable to estimate the central value and the dispersion for the quantities of interest.

It is generally accepted, [31] and [32], that the function describing the fragility of a structure, the *fragility function*, dependent on a parameter of the capacity or the demand, is the log-normal cumulative distribution function. As a result, the central value  $\theta$  and the dispersion  $\beta$  for each limit state are given in Eqs. (1) and (2) respectively, [32].

$$\theta = e^{\left(\frac{1}{N} \sum_{j=1}^N \ln z_j\right)} = \left(\prod_{j=1}^N z_j\right)^{\frac{1}{N}} \approx z_{50\%} \quad (1)$$

$$\beta = \sqrt{\frac{1}{N-1} \sum_{j=1}^N \left(\ln\left(\frac{z_j}{\theta}\right)\right)^2} \quad (2)$$

Where  $N$  is the total number of samples and  $z_j$  is the value of the demand (or capacity) parameter of interest for  $j=1, \dots, N$ . Eq. (1) shows that  $\theta$  is the geometric mean of the demand parameter  $z$  which is approximately the value of  $z$  exceeded by 50% of the data, i.e. the median value. In Eq. (2),  $\beta$  is the logarithmic standard deviation of the quantity of interest.

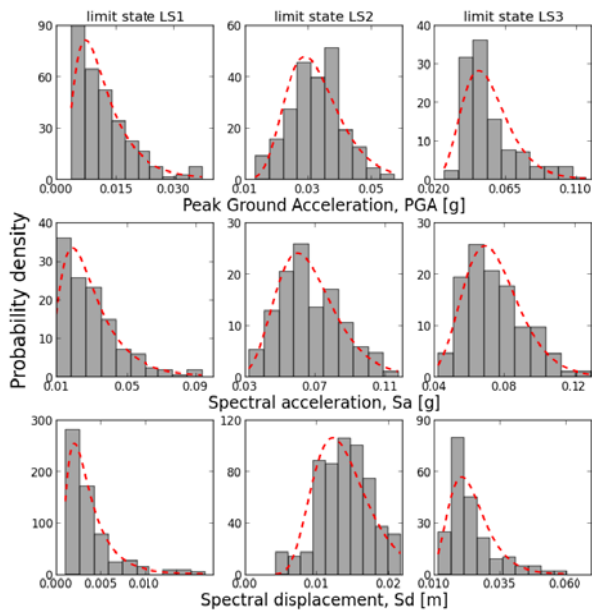


Figure 9. Histograms of the result variables and corresponding log-normal probability density functions.

The assumption that the result variables are log-normally distributed is verified in Figure 9 where the log-normal probability density function with parameters  $\ln(\theta)$ , and  $\beta$  matches the corresponding histograms with fair accuracy. In addition to that, the positive skewness of the  $S_a$  values identified in Section 4.1, is also evident in the PGA and  $S_a$  values of the different limit states in Figure 9.

#### 4.3 Fragility assessment

Finally,  $\theta$  and  $\beta$  are used to determine the fragility function shown in Eq. (3) [32].

$$P[LSi | Z] = F_i(Z) = \Phi\left(\frac{\ln(Z/\theta_i)}{\beta_i}\right) \quad (3)$$

Where  $F_i(Z)$  is the conditional probability that the structure will reach the limit state  $LSi$  or a more severe limit state as a function of the demand parameter  $Z$  and  $\Phi$  denotes the standard normal (Gaussian) cumulative distribution function.

The fragility curves in terms of peak ground acceleration, spectral acceleration and displacement are presented in Figure 10, Figure 11 and Figure 12 respectively. In Figure 10 the vertical line for PGA = 0.04 g refers to the earthquake demand of the municipality of Vimbodi and Poblet according to the Spanish code [33]. Interestingly, this demand is sufficient to produce the cracking in the vault of the main nave, since a cumulative probability of almost 100% is reached for LS1. It is worth noting that such damage is visible today, suggesting that past earthquakes, documented after historical investigation, may have left some evidences over the church. For the same earthquake demand, serious damage (LS2) is possible with a probability of 80%.

These results prove the high vulnerability of similar Romanesque structures that can be attributed to their construction typology: the large weight over the barrel vault and the irregularity in elevation due to different heights of central and lateral naves.

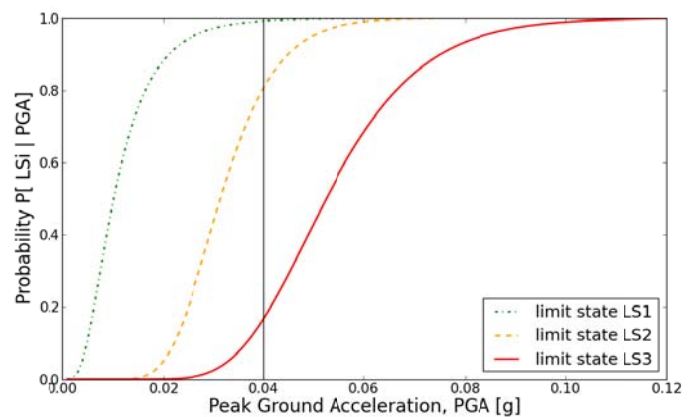


Figure 10. Fragility curves for the different limit states in terms of PGA.

It is noted, however, that the collapse of the structure (LS3) for the earthquake demand of the area is denoted by a comparatively low probability (18%). This can imply that a strengthening intervention can be dismissed at the present time, since it is not urgent. On the contrary, it would be

recommendable a better in-situ investigation on masonry members and materials, like the infill of the lateral vaults. Such activity would sufficiently limit the variation in the mechanical properties of materials.

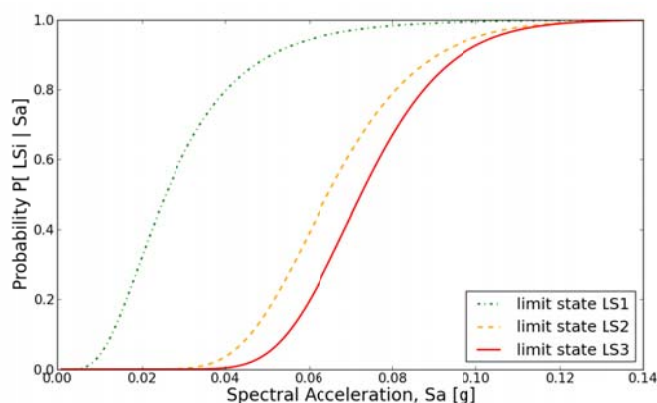


Figure 11. Fragility curves for the different limit states in terms of horizontal acceleration.

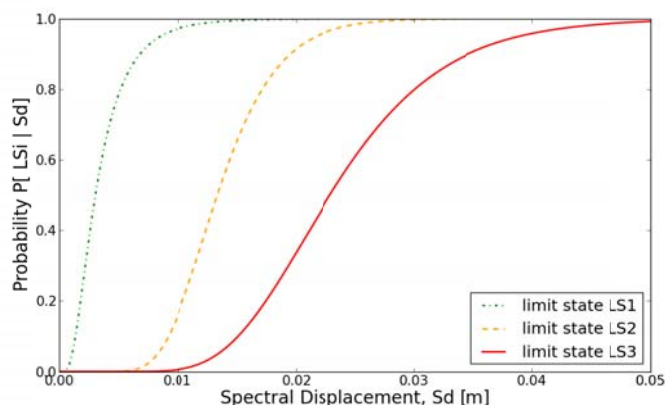


Figure 12. Fragility curves for the different limit states in terms of horizontal displacement.

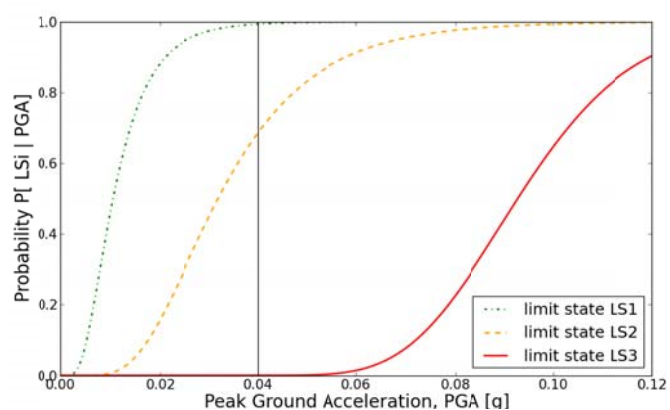


Figure 13. Fragility curves for the different limit states in terms of PGA for control point on the top of the northern pier.

As it is implied in the N2 Method, the selection of the control point in the top of the structure arises from the hypothesis that this is usually the point with the higher displacement, e.g. in frame buildings. In the study of masonry buildings this may not be the case. In the specific study, the northern springing of the barrel presents a significantly higher displacement

compared to the top of the structure. Figure 13 presents the fragility curves in terms of PGA for the capacity curves obtained having as control point the top of the northern pier. As it is visible by comparing to Figure 10, the choice of the control point affects significantly the results concerning to the collapse capacity of the structure. The selection of the optimum control point in the seismic analysis of masonry structures is still a topic under investigation, see [34], and consequently the analysts should carefully evaluate the most representative result for each studied case separately.

## CONCLUSIONS

This paper has presented a study over the seismic vulnerability of an important historical construction, the church of the Poblet Monastery, including uncertainty on structural parameters. A 2D model, including the actual deformed geometry of the most vulnerable part of the structure, was developed and studied in terms of a pushover analysis. The uncertain material properties were considered as random variables and three important limit states were defined to represent different damage thresholds of the structure. The variability of the structure's resistance against seismic actions, expressed in terms of fragility curves for the different limit states, shows that for the seismic hazard of the area the structure would present, in case of earthquake, significant damage but with low probability of collapse.

The current study showed some limitations of the N2 method applied to masonry structures. In particular, the choice of the control node for the capacity curves affects significantly the estimation of the seismic performance of the investigated structure. Therefore, the aim of future studies should focus in a more adequate methodology for the determination of the target displacement for masonry structures.

## ACKNOWLEDGMENTS

The authors wish to thank Prof. Pere Roca for his advice during the research and Jorge Portal for the drawings of the church of the Poblet Monastery.

## REFERENCES

- [1] S. Saloustros, *Structural analysis of the church of the Poblet Monastery*, Master thesis, Technical University of Catalonia, Barcelona, Spain, 2013.
- [2] NIKER, *Inventory of earthquake-induced failure mechanisms related to construction types, structural elements, and materials: Annex 1 – damage abacus*, Politecnico do Milano, Milan, Italy 2010.
- [3] P. B. Lourenço, *Analysis of historical constructions: From thrust-lines to advanced simulations*, In: Proceedings of the 3<sup>rd</sup> International Seminar in Historical Constructions, Guimarães, Portugal, pp. 91 – 116, 2001.
- [4] R. Clemente, *Análisis estructural de edificios históricos mediante modelos localizados de fisuración*, Ph.D. thesis, Technical University of Catalonia, Barcelona, Spain, 2006 [in Spanish].
- [5] P.B. Lourenço, S. Mourão, *Safety assessment of Monastery of Jerónimos, Lisbon*, In: P.B. Lourenço, P. Roca (eds) Historical Constructions, University of Minho, Guimarães, Portugal, 2001.
- [6] P.B. Lourenço, D.V. Oliveira, S. Mourão, *Numerical analysis as a tool to understand historical structures. The example of the Church of Outeiro*. In: G. Arun, N. Seçkin (eds) Studies in Ancient Structures, pp. 355-364, Yildiz Technical University, Istanbul, Turkey, 2001
- [7] UNI ENV 1998-1 (Eurocode 8), *Design of structures for earthquake resistance, Part 1: General rules, seismic actions and rules for buildings*, December 2003.
- [8] Ordinanza P.C.M. 3274, *Primi elementi in materia di criteri generali per la classificazione sismica del territorio nazionale e di normative*

- tecniche per le costruzioni in zona sismica*, Release 9/9/2004 [in Italian].
- [9] FEMA 440, *Improvement of nonlinear static seismic analysis procedures*, Federal Emergency Management Agency, Washington (DC), June 2005.
- [10] M. Cervera, L. Pelà., R. Clemente, P. Roca, *A crack-tracking technique for localized damage in quasi-brittle materials*, Engineering fracture mechanics, vol. 77, pp. 2431-50, 2010.
- [11] P. Roca, M. Cervera, L. Pelà, R. Clemente, M. Chiumenti, *Continuum FE models for the analysis of Mallorca Cathedral*, Engineering Structures, vol. 46, pp. 653-670, 2013.
- [12] GiD: the personal pre and post-processor. Barcelona: CIMNE, Technical University of Catalonia, Barcelona, Spain, 2002. <http://gid.cimne.upc.es>
- [13] M. Cervera, C. Agelet de Saracibar, M. Chiumenti, *COMET: COupled MEchanical and thermal analysis – data input manual version 5.0. Technical report IT-308*, CIMNE, Technical University of Catalonia, Barcelona, Spain, 2002.
- [14] S. Lagomarsino and S. Giovinazzi, *Macro seismic and mechanical models for the vulnerability and damage assessment of current buildings*, Bull. Earthq. Eng., vol. 4, pp. 415-443, 2006.
- [15] G. Grünthal, *European Macro seismic Scale EMS-98, vol. 15*, Centre Européen de Géodynamique et de Séismologie, Luxembourg, 1998.
- [16] K. Lang and H. Bachmann, *On the Seismic Vulnerability of Existing Buildings: A Case Study of the City of Basel*, Earthq. Spectra, vol. 20, pp. 43-66, 2004.
- [17] Karbassi and P. Lestuzzi, *Fragility Analysis of Existing Unreinforced Masonry Buildings through a Numerical-based Methodology*, vol. 6, pp. 121-130, 2012.
- [18] J. Irizarry, S. Podestà, S. Resemini, *Capacity curves of monumental-heritage elements: The Santa Maria del Mar Church in Barcelona*, In: Proceeding of international conference on earthquake loss estimation and risk reduction, 2002.
- [19] G. Martínez, P. Roca, O. Caselles, J. Clapés, *Characterization of the dynamic response for the structure of Mallorca cathedral*. In: Proceeding of 5th international conference on structural analysis of historical constructions, 2006
- [20] P.I.E.T 70, *Prescripciones del instituto Eduardo Torroja*, Madrid, 1971 [in Spanish]
- [21] Italian Ministry of Infrastructure and Transport, *Circolare 2 Febbraio 2009, n. 617. Istruzioni per l'applicazione delle nuove norme tecniche per le costruzioni*, 2009 [in Italian].
- [22] B. Möller and M. Beer, *Engineering computation under uncertainty-capabilities of non-traditional models*, Computers & Structures, vol. 86, pp. 1024-1041, 2008.
- [23] W. Graf, M. Götz, M. Kaliske., *Analysis of dynamical processes under consideration of polymorphic uncertainty*, In: Proceedings of 11th International Conference on Structural Safety & Reliability, Columbia University New York, 2013.
- [24] G. Kokolakis and I. Spiliotis, *Introduction to Probability theory and Statistics*, Simeon Editions, Athens, 4th edition, 1999 [in Greek].
- [25] Singhal and A. Kiremidjian, *Method for Probabilistic Evaluation of Seismic Structural Damage*, Journal of Structural Engineering, vol. 122, pp. 1459-1467, 1996.
- [26] Dymiotis, A. Kappos, M. Chryssanthopoulos, *Seismic Reliability of RC Frames with Uncertain Drift and Member Capacity*, Journal of Structural Engineering, vol. 125, 1038-1047, 1999.
- [27] M. D. McKay, R. J. Beckman, W. J. Conover, *A Comparison of Three Methods for Selecting Values of Input Variables in the Analysis of Output from a Computer Code*, Technometrics, vol. 21, pp. 239-245, 1979.
- [28] R. L. Iman, *Latin Hypercube Sampling*. Encyclopedia of Quantitative Risk Analysis and Assessment, 2008.
- [29] D. Vamvatsikos M. and Fragiadakis, *Incremental dynamic analysis for estimating seismic performance sensitivity and uncertainty*, Earthquake Engng. Struct. Dyn., vol. 39, pp. 141-163, 2010.
- [30] F. Jalayer, I. Iervolino, G. Manfredi, *Structural modeling uncertainties and their influence on seismic assessment of existing RC structures*, Structural Safety, vol. 32, pp. 220-228, 2010.
- [31] Federal Emergency Management Agency, *HAZUS-MH MR4: Technical Manual*, Vol. Earthquake Model, Washington DC, 2010.
- [32] ATC-58, *Guidelines for Seismic Performance Assessment of Buildings*, Applied Technology Council, Redwood City, California, 2009.
- [33] Comisión Permanente de Normas Sismo resistentes, *Norma de construcción sismo resistente NCSE-02, Real Decreto 997/2002*, Spanish Ministry of Public Works, Madrid, Spain, 2002 [in Spanish].
- [34] L. Pelà, A. Aprile, A. Benedetti, *Comparison of seismic assessment procedures for masonry arch bridges*, Construction and Building Materials vol. 38, pp. 381-394, 2013.